Coherent deflection of atomic samples and positional mesoscopic superpositions

L. F. Alves da Silva, L. M. R. Rocha, and M. H. Y. Moussa.

Instituto de Física de São Carlos, Universidade de São Paulo,

P.O. Box 369, São Carlos, 13560-970, São Paulo, Brazil

Abstract

We present a protocol based on the interplay between superradiance and superabsorption to achieve the coherent deflection of an atomic sample due to the momentum transfer from the atoms to a cavity field. The coherent character of this momentum transfer, causing the atomic sample to deflect as a whole, follows from the collective nature of the atomic superradiant pulse and its superabsorption by the cavity field. The protocol is then used for the construction of positional mesoscopic atomic superpositions.

The optical Stern-Gerlach effect —the splitting of the trajectory of an on- or off-resonant two-level atom by a quantized electromagnetic field—, dates to the late 1970s [1, 2] and early 1980s [3], and its experimental demonstration occurred in the early 1990s [4]. Knowing that the photon statistics of a cavity field can manifest itself in the momentum distribution of the scattered atoms [5], the optical Stern-Gerlach was used for quantum nondemolition measurement of photon statistics [6] and for the state tomography of a cavity field [7]. Later, [8], the splitting of the atomic trajectory was considered for the proposition of a fully quantum protocol for two-dimensional atomic lithography, and also for entanglement detection from atomic deflection [9].

In the present work we propose a protocol for the coherent deflection of an atomic sample from which we can then construct, for example, a positional mesoscopic superposition. The generation of mesoscopic superpositions has been a much pursued challenge for their interface between the micro and macrophysics, allowing both the testing of fundamental quantum principles and applications in quantum technology [10, 11].

To achieve such a coherent deflection of the sample, we take advantage of three previous developments: *i*) First, the optical Stern-Gerlach effect [1–4]. *ii*) Second, the recently proposed interplay between superradiance [12] and superabsorption [13] of a moderately dense atomic sample trapped inside a cavity [14]: When preparing the N-atoms sample in a superradiant state, with the cavity field in the vacuum, the coherent pulse emitted by the sample is superabsorbed by the resonant cavity mode due to an atom-field Rabi coupling g enhanced by the factor $\sqrt{N}$. (This enhanced coupling was previously derived through a semiclassical approach [15, 16] and experimentally confirmed in what is called the ringing regime of superradiance [17].) The field excitation is then superradiated and superabsorbed back to the atomic sample in a cyclic decaying process. We demonstrate here that this superradiance-superabsorption interplay accounts for the momentum transfer between atoms and field, allowing the coherent deflection of the sample. *iii*) To know the states of the atomic sample and the cavity mode, which are necessary for computing the momentum transfer and for the construction of positional mesoscopic superpositions, we also resort to the Lewis & Riesenfeld dynamical invariants [18], as advanced in Ref. [19] for the atomic sample state, and in Ref. [20] for the field state.

As antecipated above, in Ref. [14] the authors consider a moderately dense atomic sample trapped inside a high-Q cavity, resonantly interacting with a cavity mode. The Hamiltonian of the system, $H = H_0 + H_I$, is given by ($\hbar = 1$)

$$H_0 = \omega a^\dagger a + \omega S_z + \sum_k \omega_k b_k^\dagger b_k, \tag{1a}$$

$$H_I = g\left(S_+ a + S_- a^\dagger\right) + \sum_k \lambda_k \left(S_+ b_k + S_- b_k^\dagger\right), \tag{1b}$$

with H_0 accounting for the cavity mode (described by the field creation and annihilation operators, $a^\dagger$ and a), and the atomic sample (described by the collective pseudospin operator $S_z = n\sum_{n=1}^{N}\sigma_z$). H_0 also accounts for the reservoir (described by the multimode creation and annihilation operators, $b_k^\dagger$ and b_k). H_I describes the interaction of the atomic sample, where $S_\pm = \sum_{n=1}^{N}\sigma_\pm$, with the cavity mode ($g$) and the environment ($\lambda_k$). Considering the field quadratures $X_1 = \left(a + a^\dagger\right)/2$ and $X_2 = \left(a - a^\dagger\right)/2i$, a mean-field treatment of the system reduces the Hamiltonian (1) to the nonlinear time-dependent form $H(t) = H_a(t) + H_f(t)$, with

$$H_a = \omega s_z + 2\Lambda_R\left(\langle s_x\rangle s_x + \langle s_y\rangle s_y\right) - 2\Lambda_I\left(\langle s_x\rangle s_y - \langle s_y\rangle s_x\right), \tag{2a}$$

$$H_f = \omega a^\dagger a + 2\sqrt{N}g\left(\langle s_x\rangle X_1 - \langle s_y\rangle X_2\right). \tag{2b}$$

The atomic sample is thus replaced by a representative atom, described by H_a through the operators $s_\mu = \sigma_\mu/2$, with $\mu = x, y, z$ and $\sigma_\pm = \left(\sigma_x \pm i\sigma_y\right)/2$. This atom is under a nonlinear amplification with strength $\Lambda = \Lambda_R + i\Lambda_I$, where

$$\Lambda_R = \sqrt{N}g\frac{\langle s_x\rangle\langle X_1\rangle - \langle s_y\rangle\langle X_2\rangle}{\langle s_x\rangle^2 + \langle s_y\rangle^2}, \tag{3a}$$

$$\Lambda_I = \sqrt{N}g\frac{\langle s_x\rangle\langle X_2\rangle + \langle s_y\rangle\langle X_1\rangle}{\langle s_x\rangle^2 + \langle s_y\rangle^2} - \frac{N\gamma}{2}, \tag{3b}$$

γ being the atomic decay factor. Moreover, an enhanced effective coupling $\sqrt{N}g$ emerges between the representative atom and the cavity field as described by H_f.

Starting with the atomic sample in an inverted populated state and the cavity mode in the vacuum, the environment then triggers the superradiant pulse which is superabsorbed by the mode due to the enhanced coupling. Another important feature of the nonlinear mean-field Hamiltonians H_a and H_f, is that although they commute with each other, leading to separate Schrödinger equations, $i\partial_t\left|\psi_\xi\right\rangle = H_\xi\left|\psi_\xi\right\rangle$ ($\xi = a$ or f), for initial product states $\left|\psi_a\right\rangle \otimes \left|\psi_f\right\rangle$, there is an indirect coupling between atom and field coming from the time-dependent mean values.

To solve the Schrödinger equation for the time-dependent Hamiltonians H_a and H_f, we use the Lewis & Riesenfeld dynamic invariants [18], for the atom $I_a(t)$ and the field $I_f(t)$, defined as $\partial_t I_\xi - i\left[I_\xi, H_\xi\right] = 0$. Following Refs. [19, 20], we propose the operators

$$I_a = \langle s_x\rangle s_x + \langle s_y\rangle s_y + \langle s_z\rangle s_z, \tag{4a}$$

$$I_f = a^\dagger a - 2\langle X_1\rangle X_1 - 2\langle X_2\rangle X_2 + \chi, \tag{4b}$$

to obtain the system

$$\langle \dot{s}_x\rangle = -\omega\langle s_y\rangle + 2\langle s_z\rangle\left(\Lambda_R\langle s_y\rangle - \Lambda_I\langle s_x\rangle\right), \tag{5a}$$

$$\langle \dot{s}_y\rangle = \omega\langle s_x\rangle - 2\langle s_z\rangle\left(\Lambda_R\langle s_x\rangle + \Lambda_I\langle s_y\rangle\right), \tag{5b}$$

$$\langle \dot{s}_z\rangle = \Lambda_I\left(\langle s_x\rangle^2 + \langle s_y\rangle^2\right), \tag{5c}$$

$$\langle \dot{X}_1\rangle = \omega\langle X_2\rangle - \sqrt{N}g\langle s_y\rangle, \tag{5d}$$

$$\langle \dot{X}_2\rangle = -\omega\langle X_1\rangle - \sqrt{N}g\langle s_x\rangle, \tag{5e}$$

together with the equation $\dot{\chi} = -\sqrt{N}g\left(\langle s_x\rangle\langle X_2\rangle + \langle s_y\rangle\langle X_1\rangle\right)$ that avoids unnecessary constraints on the mean values defining I_f.

From the fact that $\langle \dot{I}_a\rangle = 0$, such that $\langle I_a\rangle = \langle s_x\rangle^2 + \langle s_y\rangle^2 + \langle s_z\rangle^2 = R^2$, we consider a Bloch sphere of radius R to define the mean values $\langle s_x\rangle = R\sin\theta\cos\phi$, $\langle s_y\rangle = R\sin\theta\sin\phi$, $\langle s_z\rangle = R\cos\theta$. We then derive the eigenvectors of I_a, given by $|+,t\rangle = \cos\left(\theta/2\right)|e\rangle + e^{i\phi}\sin\left(\theta/2\right)|g\rangle$ and $|-,t\rangle = \sin\left(\theta/2\right)|e\rangle - e^{i\phi}\cos\left(\theta/2\right)|g\rangle$, where the vector $|g\rangle$ ($|e\rangle$) of the representative atom corresponds to the entire sample in the ground (excited) state. Starting from the general superposition $|\psi_a(t)\rangle = c_+|+,t\rangle + c_-|-,t\rangle$, we verify that the eigenstate $|-,t\rangle$ is rulled out of the solution of the atomic Schrödinger equation by the self-consistency condition $\langle s_z\rangle = \left[\left(|c_+|^2 - |c_-|^2\right)\cos\theta + 2\,\mathrm{Re}\left(c_+c_-^* e^{i(\Phi_+ - \Phi_-)}\right)\sin\theta\right]/2 = R\cos\theta$. For a positive defined radius $R = 1/2$, this condition leads to $|c_+| = 1$ and $|c_-| = 0$, in agreement with the self-consistency conditions for $\langle s_x\rangle$ and $\langle s_y\rangle$. We then derive the solution of the Schrödinger equation for the atom as

$$|\psi_a(t)\rangle = e^{i\Phi_+^a(t)}|+,t\rangle, \tag{6}$$

where the Lewis & Riesenfeld phase factor is given by

$$\Phi_+^a(t) = -\frac{\omega t}{2} - \int_0^t \Lambda_R \sin^2\left(\theta/2\right)dt'. \tag{7}$$

The solution for the field is reached by defining $\alpha = \langle a\rangle$ [20], with $\dot{\alpha} = -i\left[\omega\alpha + \left(\sqrt{N}g/2\right)\sin\theta e^{-i\phi}\right]$, in agreement with Eqs. (5d) and (5e). Starting with the field in the coherent state α_0, we then obtain

$$|\psi_f(t)\rangle = e^{i\Phi^f(t)}|\alpha(t)\rangle, \tag{8}$$

with the Lewis & Riesenfeld phase

$$\Phi^f(t) = \int_0^t \left[\omega\,|\alpha|^2 - \frac{\sqrt{N}g}{4}\left(\alpha e^{i\phi} + \alpha^* e^{-i\phi}\right)\sin\theta\right] dt'. \tag{9}$$

After computing the system state vector

$$|\psi(t)\rangle = e^{i\left[\Phi^a_+(t)+\Phi^f(t)\right]}|+,t\rangle \otimes |\alpha(t)\rangle, \tag{10}$$

we are now able to approach the coherent deflection of the atomic sample, starting with some considerations on the experimental implementation of the process. We must assume that the trapped sample, with the atoms initially in their ground states, is placed near a node of the standing-wave field as in [7], for a greater atomic momentum transfer, proportional to the gradient of the cavity field [21]. Then, by manipulating the convexity of the trap potential, a moderately dense atomic sample is built. The initial state of the sample is then immediately prepared in the superposition $|\psi_a(0)\rangle = \cos[\theta_0/2]\,|e\rangle + e^{i\phi}\sin[\theta_0/2]\,|g\rangle$ [22]. Right after the preparation of the state $|\psi_a(0)\rangle$, the trap potential is turned off and the sample starts to interact with the cavity while leaving it under gravity. Alternatively we can consider a sample of ions accelerated by an electric field which is turned on immediately after the radiation-matter interaction. Starting from the cavity mode in the vacuum, we thus have the initial state $|\psi(0)\rangle = |+,0\rangle \otimes |0\rangle$, which evolves exactly to $|\psi(t)\rangle$ in Eq. (10).

For computing $\theta(t)$, $\phi(t)$ and $\alpha(t) = |\alpha(t)|\,e^{i\phi_\alpha(t)}$ from Eqs. (5), we consider the condition $\omega_0 \gg N\gamma, \sqrt{N}g$. We then derive the solution $\phi(t) \approx \pi/2 - \phi_\alpha(t) \approx \phi_0 + \omega t$, where $\tan\phi_\alpha = \langle X_2\rangle/\langle X_1\rangle \approx \tan(\pi/2 - \phi)$, and the Lienard system

$$\frac{d\theta}{dt} = \frac{N\gamma}{2}\sin\theta - 2\sqrt{N}g\,|\alpha|\,, \tag{11a}$$

$$\frac{d\,|\alpha|}{dt} = -\frac{\sqrt{N}g}{2}\sin\theta, \tag{11b}$$

leading to the Lienard equation

$$\ddot{\theta} = \frac{N\gamma}{2}\cos(\theta)\,\dot{\theta} + (\sqrt{N}g)^2\sin\theta, \tag{12}$$

which helps us to define, regarding the parameter $\epsilon = 4\sqrt{N}g/N\gamma$, three regimes for solutions of our superradiance-superabsorption interplay: the overdamped ($\epsilon \ll 1$), the damped

($\epsilon \approx 1$), and the underdamped ($\epsilon \gg 1$) regimes. We first consider the overdamped regime where an approximated analytic solution can be obtained from Eqs. (11), which also applies, with much less accuracy, for the damped regime. In this regime the superradiant-superabsorption cycle begin to emerge, indicating that the excitation superradiated by the sample is superabsorbed by the cavity field, ensuring the momentum transfer between radiation and matter. We then consider the underdamped regime where the momentum transfer is fully accomplished.

i) The overdamped regime. For the overdamped regime, the perturbative parameter ϵ allows us to consider the first order expansions $\theta(t) \approx \theta_h(t) + \epsilon\vartheta(t)$ and $|\alpha(t)| \approx \alpha_h(t) + \epsilon\tilde{\alpha}(t)$. The solutions $\sin\theta_h(t) = \text{sech}\left[(t-\tau_D)/\tau\right]$ [19] and $\alpha_h(t) = \alpha_0$, arise from the homogeneous equations resulting when we turn off the atom-field coupling, such that $\epsilon = 0$. To be computed below, τ_D is the delay time for the initial atomic state $|\psi_a(0)\rangle$ to evolve to the well-known superradiant superposition $\left(|e\rangle + e^{i\phi}|g\rangle\right)/\sqrt{2}$ [17], whereas $\tau = 2/N\gamma$ is the characteristic emission time of the free-sample Dicke's superradiance. These approximations reduce the Lienard system to the decoupled equations $\dot{\vartheta} = (N\gamma/2)\left(\vartheta\cos\theta_h - 4\alpha_h\right)$ and $\dot{\alpha} = -(N\gamma/2)\sin\theta_h$, leading to the solutions

$$\theta(t) \approx \theta_h(t) + \alpha_0\epsilon\cos\theta_h(t), \tag{13a}$$

$$|\alpha(t)| \approx \alpha_0 + (\epsilon/4)\left[\theta_h(t) - \theta_0\right], \tag{13b}$$

where we have assumed $\theta(\tau_D) = \theta_h(\tau_D) = \pi/2$ and $\alpha(0) = \alpha_h(0) = \alpha_0$, such that $\vartheta(\tau_D) = 0$ and $\tilde{\alpha}(0) = 0$. We have also assumed $\phi_0 = \pi/2$ leading to $\phi_\alpha(0) = 0$ and $\alpha(0) = |\alpha(0)| = \alpha_0$. From Eq. (13a) we derive the expression

$$e^{\frac{\tau_D}{\tau}}\tan\frac{\theta_0}{2} + \alpha_0\epsilon\left(\tan\frac{\theta_0}{2} - \sinh\frac{\tau_D}{\tau}\right)\tanh\frac{\tau_D}{\tau} \approx 1, \tag{14}$$

which enables us to compute the delay time τ_D. Starting from the superradiant state with $\theta_0 = \pi/2$, we verify, as expected, that $\tau_D = 0$. For $\theta_0 \ll 1$ we may assume that $\tau_D/\tau \gg 1$, leading us from Eq. (14) to

$$\tau_D \approx \tau\ln\left|\frac{\cot(\theta_0/2) - \alpha_0\epsilon}{1 - \alpha_0(\epsilon/2)\cot(\theta_0/2)}\right|, \tag{15}$$

showing that for $\epsilon = 0$ we retrieve the well-known result for the Dicke's superradiance: $\tau_D \approx \tau\ln\cot(\theta_0/2)$.

ii) The underdamped regime. Back to the Lienard equation (12), we now linearize the senoidal functions around $\theta = \pi$, to retrieve the standard solution for an underdamped oscillator, given by

$$\theta(t) \approx \pi - \left[(\pi - \theta_0)\cos\left(\sqrt{N}gt\right) + 2\alpha_0 \sin\left(\sqrt{N}gt\right)\right] e^{-N\gamma t/4}, \tag{16}$$

with $|\alpha(t)|$ following by substituting Eq. (16) into Eq. (11b). We note that the solutions in Eq. (13) could also have been derived from the linearization proceedure around $\theta = \pi$ and $\alpha = 0$, but under the restriction that the initial condition is far from the metastable point $\theta_0 = 0$.

With the above solutions in Eqs. (13) and (16), we analyze the evolution of the system state vector in Eq. (10), where we now consider the position dependence of the atom-field coupling $g(x) = \mu\mathcal{E}\sin(kx)$, with μ, $\mathcal{E}$ and k standing respectively for the atomic dipole moment, the effective electric field per photon, and the wave-vector of the cavity mode. As already anticipated, we assume that the trapped sample is placed on a node of the cavity field, such that $g(x) \approx \mu\mathcal{E}kx$, remembering that the superradiant sample must be small compared to the wavelength of the superabsorptive mode.

Starting from the initial state vector of the system

$$|\psi(x, t = 0)\rangle = \int_{-\infty}^{+\infty} \Theta(x)|+, 0\rangle \otimes |\alpha_0\rangle \otimes |x\rangle dx, \tag{17}$$

with $\Theta(x)$ standing for the spatial distribution of the atomic sample, we obtain after the interaction time t,

$$|\psi(x, t)\rangle = \int_{-\infty}^{+\infty} e^{+i\left[\Phi_+^a(x,t)+\Phi^f(x,t)\right]}\Theta(x)|+, t\rangle \otimes |\alpha(x, t)\rangle \otimes |x\rangle dx, \tag{18}$$

now considering that the field coherent state also depends upon the Rabi frequency $g(x)$. The Raman-Nath regime —by which the kinetic energy of the sample is neglected, by assuming that its transverse displacement along the interaction time is small compared to the wavelength of the mode— is here perfectly observed since the sample is released from the trap with zero velocity. From the state vector in Eq. (18), we next analyse the momentum transfer for the overdamped and the underdamped regimes, considering the solutions $\Phi_+^a(t) = -\omega t/2$ and $\Phi^f(t) = 0$ valid whatever the regime.

i) The overdamped regime. By projecting the state $|\psi(x, t)\rangle$ onto the position space, we obtain the solution

$$|\psi(x, t)\rangle = \frac{e^{-i\omega t/2}}{\sqrt{2}}\Theta(x)\left[e^{i\theta_h(t)/2}e^{ikx\kappa(t)}|+, t) + e^{-i\theta_h(t)/2}e^{-ikx\kappa(t)}|-, t)\right] \otimes |\alpha(x, t)\rangle, \tag{19}$$

where we have defined the effective interaction parameter

$$\kappa(t) = \frac{2\mu\mathcal{E}\alpha_0}{\sqrt{N}\gamma}\tanh\left(\frac{t-\tau_D}{\tau}\right), \tag{20}$$

and considered the expansion $|+,t\rangle = \left[e^{i\theta(x,t)/2}|+,t) + e^{-i\theta(x,t)/2}|-,t)\right]/\sqrt{2}$, with $|\pm,t) = \left(|e\rangle \pm e^{i\phi(t)}|g\rangle\right)/\sqrt{2}$. The sample-field momentum transfer $k\kappa(t)$ may be alternatively computed from $\Delta\dot{p} = \sqrt{N}\vec{\mu}.\nabla\vec{E}$, where $\vec{E} = \mathcal{E}\alpha(t)\sin(kx)\hat{\mu}$ and $\sqrt{N}\vec{\mu}$ is an effective dipole moment. Then, it follows the rate $\kappa = \Delta p/k = \sqrt{N}\mu\mathcal{E}\alpha_0\Delta t$ which, for time intervals around the characteristic emission time $\tau = 2/N\gamma$, leads to $\kappa = \Delta p/k = 2\mu\mathcal{E}\alpha_0/\sqrt{N}\gamma$, in agreement with Eq. (20).

It is well-known in Dicke's superradiance that $\theta_0 = 0$ implies a metastable state of the atomic sample, of infinitely long duration. Here, as we conclude from the Lienard Eqs. (11), a metastable state of the radiation-matter system occurs for $\alpha_0 = 0$ and $\theta_0 = 0$. Regarding α_0, we emphasize that our experiment does not require a high finesse cavity as far as the necessary superradiant-superabsorption cycle occurs in a short time interval of the order of $\tau_D + \tau \ll 1/\gamma$. However, the cavity must be cooled so that the initial average excitation of the field, α_0, is small enough to ensure $\alpha_0\epsilon \ll 1$. Regarding the atomic variable θ_0, we may consider, as an approximation, the result $\tau_D \approx \tau\ln\left[\cot(\theta_0/2)\right] \approx \tau\ln N$ from Dicke's superradiance [12], to infer that $\theta_0 \approx 2/N$.

For a time interval around $\tau_D+\tau$, such that $\tanh\left[(t-\tau_D)/\tau\right] \approx 1$ and $\kappa(t) \approx 2\mu\mathcal{E}\alpha_0/\sqrt{N}\gamma$, it is reasonable to disregard the dependence on position of the field state $\alpha(x,t)$, once the cavity field superabsorption has already been established. After Fourier transforming the state vector $|\psi(x,t)\rangle$ over the momentum representation, it follows that

$$|\psi(p,t)\rangle = \frac{1}{\sqrt{2}}\left[e^{-i\phi_+(t)}\mathcal{F}\left[p-k\kappa(t)\right]|+,t) + e^{-i\phi_-(t)}\mathcal{F}\left[p+k\kappa(t)\right]|-,t)\right] \otimes |\alpha(t)\rangle, \tag{21}$$

with $\phi_\pm(t) = \left[\omega t \pm \theta_h(t)\right]/2$ and the amplitude

$$\mathcal{F}(p) = \frac{1}{\sqrt{2\pi}}\int_{-\infty}^{+\infty} e^{-ipx}\Theta(x)\,dx, \tag{22}$$

is the Fourier transform of the atomic spatial distribution. Eq. (21) shows that the sample is coherently deflected with momentum $\pm k\kappa(t)$ in the states $|\pm,t)$.

ii) The underdamped regime. By inserting the solution 16 into Eq. 18 projected onto the position space, we obtain the Fourier transform

$$|\psi(p,t)\rangle = \left[e^{-i\omega t/2}\mathcal{F}_-(p)|e\rangle + ie^{i\omega t/2}\mathcal{F}_+(p)|g\rangle\right] \otimes |\alpha(t)\rangle, \tag{23}$$

where, using $R(t) \approx \sqrt{(\theta_0-\pi)^2/4+\alpha_0^2 e^{-N\gamma t/4}}$ and $\tan\varphi = 4\alpha_0/\pi$, we obtain

$$\mathcal{F}_{\pm}(p) = \frac{i}{\sqrt{8\pi}} \int_{-\infty}^{+\infty} e^{-ipx}\Theta(x)\left(e^{-iR(t)\cos\left(\sqrt{N}\mu\mathcal{E}kxt+\varphi\right)} \pm e^{iR(t)\cos\left(\sqrt{N}\mu\mathcal{E}kxt+\varphi\right)}\right) dx, \tag{24}$$

From the Bessel identity [23]

$$e^{\pm iR\cos\zeta} = \sum_{n=-\infty}^{\infty} (\pm i)^n J_n(R)\, e^{\mp in\zeta}, \tag{25}$$

and considering $R(t) \ll 1$, in accordance with the linearization procedure, we finally obtain

$$\mathcal{F}_{+}(p) \approx iJ_0(R)\,\mathcal{F}(p), \tag{26a}$$

$$\mathcal{F}_{-}(p) \approx J_{+1}(R)\left[e^{i\varphi}\mathcal{F}\left(p-\sqrt{N}\mu\mathcal{E}kt\right)+e^{-i\varphi}\mathcal{F}\left(p+\sqrt{N}\mu\mathcal{E}kt\right)\right], \tag{26b}$$

with $J_0(R) = 1-(R/2)^2$, $J_{+1}(R) = -J_{-1}(R) \approx R/2$. From Eqs. (26) we verify the splitting of the whole incident sample into three different paths. The undeflected path is associated with the representative state $|g\rangle$ whereas the deflected ones, with momenta $\pm\sqrt{N}\mu\mathcal{E}kt$, are associated with $|e\rangle$:

$$|\psi(p,t)\rangle \approx \left\{ i\mathcal{F}(p)\,|g\rangle + (R/2)\left[e^{i\varphi}\mathcal{F}\left(p-\sqrt{N}\mu\mathcal{E}kt\right)+e^{-i\varphi}\mathcal{F}\left(p+\sqrt{N}\mu\mathcal{E}kt\right)\right]|e\rangle \right\} \otimes |\alpha(t)\rangle. \tag{27}$$

We observe that the momentum transfer is that of a single atom [7] multiplied by the factor $\sqrt{N}$, which is larger the longer the sample-field interaction time, i.e., the larger the number of superradiance-superabsorptive cycles. If on the one hand the momentum transfer increases with time, on the other the measurement probability of the deflected sample decreases as a function of the damping function $R(t)$.

Next, for both the overdamped and the underdamped regimes, we must characterize the superradiant-superabsorption cycles and estimate the magnitude of the sample-field momentum transfer. Considering the energies of the representative atom and the cavity field, given by $\varepsilon_a = \omega_0\langle\sigma_z\rangle/2$ and $\varepsilon_f = \omega_0\left\langle a^\dagger a\right\rangle$, we compute the complementary intensities $\mathcal{I}_a$ and $\mathcal{I}_f$ [14]:

$$\mathcal{I}_a = -N\frac{d\varepsilon_A}{dt} = N\omega_0|\langle\sigma_-\rangle|\left[N\gamma|\langle\sigma_-\rangle| + 2\sqrt{N}g\sin(\phi_\sigma-\phi_a)|\langle a\rangle|\right], \tag{28a}$$

$$\mathcal{I}_f = -N\frac{d\varepsilon_F}{dt} = N^2\gamma\omega_0|\langle\sigma_-\rangle|^2 - \mathcal{I}_A. \tag{28b}$$

Thus, starting with the overdamped regime with $\gamma = 4 \times 10^{-2} g$, such that $\epsilon = 0.1$, in Fig. 1(a, b, and c) we present the curves for the numerical and analytical solutions for $\theta(t)$, $|\alpha(t)|$, $\mathcal{I}_a$ and $\mathcal{I}_f$, respectively. Wheres the circles and squares represent the numerical solutions, the full and dotted lines represent the analytical ones. We have assumed a mesoscopic sample with $N = 10^6$, and in accordance with the consideration made above: $\omega = 10^5 g$, $\alpha_0 = 0.1$, $\theta_0 = 2/N$ and $\phi_0 = \pi/2$. As we observe, the analytical solutions match very well for the overdamped regime where we basically observe, in Fig. 1(c), an atomic superradiant pulse with intensity of about $10^{15} g^2$ and delay time $\tau_D \approx 2.65 \times 10^{-4} g^{-1}$, in perfect agreement with the analytical value coming from Eq. 15. The field superabsorption, presenting negative intensities [14], is inhibited by the large atomic decay factor. In Fig. 2(a, b, and c), we consider the same functions as in Fig. 1 for the damped regime with $\gamma = 4 \times 10^{-3} g$ and $\epsilon = 1$, with all other parameters equal to those in Fig. 1. As antecipated above, our overdamped solutions apply with much less accuracy to the damped regime. We now observe a superradiant-superabsorption cycle, although the superabsorption occurs slightly less intensely than the superradiance ($10^{14} g^2$). Moreover, the delay time for superabsorption is slightly greater than that for the superradiance, the latter being around $\tau_D \approx 1.45 \times 10^{-3} g^{-1}$.

In Fig. 3(a, b, and c), we consider the underdamped regime with $\gamma = 4 \times 10^{-4} g$ and $\epsilon = 10$, and again all other parameters equal to those in Fig. 1, except for $\theta_0 = \pi/2$ due to the linearization procedure. Now, we observe around 8 superradiant-superabsorption cycles, with intensities starting at around $10^{14} g^2$, as the weak dissipative rate leads to a slow damping of the initial atomic excitation. The number of superradiance-superabsorption cycles can be controlled by Stark shifting the sample out of ressonance with the field. From Ref. [14] it follows that the time interval for a superradiant-superabsorption cycle is around $2/\sqrt{N} g$, which is in agreement with Fig. 3(c).

We finally address the magnitude of the sample-field momentum transfer, assuming that the atomic spatial distribution is a narrow Gaussian centered around the node, $\Theta(x) = \exp\left[-x^2/2\sigma^2\right]/\sqrt{2\pi}\sigma$, of small enough width σ, such that $k\sigma \ll 1$. Considering, for the damped regime, the spatial distribution of the atomic sample of width $\sigma \approx 0.2/k$ and the parameters used in Fig. 2, we obtain a momentum transfer for the deflected atoms in states $|\pm, t)$ around that of a cavity-field photon: $\Delta p \approx \pm k$. This magnitude is considerably smaller than the momentum uncertainty around $1/\sigma \approx 5k$. However the momentum transfer is significantly increased in the underdamped regime where a numerical account for the momentum distributions in Eq. (26) is shown in Fig. 4 against the scaled interaction time $\sqrt{N}gt$. The distributions $|\mathcal{F}_+|^2$ and $|\mathcal{F}_-|^2$ are represented by the green and red curves, respectively. We have considered the same parameter as in Fig. 3, with $\sigma \approx 0.2/k$, to observe that the momentum for $t = 6/\sqrt{N}g$ is around $50k$, far greater than the momentum uncertainty. As stated above, this momentum transfer is evidently greater the longer the sample-field interaction time.

Therefore, the use of the interplay between superradiance and superabsorption, advanced in Ref. [14], proves to be a suitable tool to achieve a coherent deflection of an atomic sample and consequently to achieve a long-sought goal: the preparation of momentum (or positional) mesoscopic superpositions. We stress that superradiant Rayleigh scattering from a Bose-Einstein condensate has been used to produce superpositions of (stationary) momentum states of recoiled atoms [24]. Such superpositions, created by the density modulation of the condensate and consequently the Bragg scattering regime, are different in nature from that in Eq. 27, where the momentum increases with time as observed in Fig. 4.

The present proposal poses a challenge to the experimental physics of radiation-matter interaction, seeking to extend the remarkable advances achieved in the last 4 decades [11] to the domain of many-body physics. This has, in fact, already begun with the coupling of a Bose-Einstein condensates with a cavity field to achieve the Dicke quantum phase transition [25] and to enhanced superradiant Rayleigh scattering [26]. In particular, we observe that the present development, together with Ref. [14], can be used for the proposition of a more efficient quantum lithography protocol based on the deflection of atomic samples instead of individual atoms as in Ref. [8]. It can also be used for the construction of positional mesoscopic atomic entanglements, and for the implementation of quantum processing with mesoscopic ensembles, a goal that has been pursued since the early 2000s [27].

Acknowledgements

The authors acknowledge financial support from CNPQ and CAPES, Brazilian agencies.

---

[1] A. P. Kazantsev, Zh. Eksp. Teor. Fiz. **67**, 1660 (1975) [Sov. Phys. JEPT **40**, 825 (1975)]; A. P. Kazantsev, Usp. Fiz. Nauk **124**, 113 (1978) [Sov. Phys. Usp. **21**, 58 (1978)].

[2] R. J. Cook, Phys. Rev. Lett. **41**, 1788 (1978).

[3] C. Tanguy, S. Reynaud, and C. C. Tannoudji, J. Phys. B **17**, 4623 (1984).

[4] T. Sleator, T. Pfau, V. Balykin, O. Carnal, and J. Mlynek, Phys. Rev. Lett. **68**, 1996 (1992).

[5] V. M. Akulin, F. L. Kien, and W. P. Schleich, Phys. Rev. A **44**, R1462 (1991).

[6] A. M. Herkommer, V. M. Akulin, W. P. Schleich, Phys. Rev. Lett. **69**, 3298 (1992).

[7] M. Freyberger and A. M. Herkommer, Phys. Rev. Lett. **72**, 1952 (1994); M. H. Y. Moussa, S. S. Mizrahi, and A. O. Caldeira, Phys. Lett. A **221**, 145 (1996).

[8] C. E. Máximo, T. B. Batalhão, R. Bachelard, G. D. de Moraes Neto, M. A. de Ponte, and M. H. Y. Moussa, JOSA B **31**, 2480 (2014).

[9] C. E. Máximo, R. Bachelard, G. D. de Moraes Neto, and M. H. Y. Moussa, JOSA B **34**, 2452 (2017).

[10] D. Leibfried, E. Knill, S. Seidelin, J. Britton, R. B. Blakestad, J. Chiaverini, D. B. Hume, W. M. Itano, J. D. Jost, C. Langer, R. Ozeri, R. Reichle and D. J. Wineland, Nature **438**, 639 (2005); B. Vlastakis, G. Kirchmair, Z. Leghtas, S. E. Nigg, L. Frunzio, S. M. Girvin, M. Mirrahimi, M. H. Devoret, R. J. Schoelkopf, Science **342**, 607 (2013); A. Facon, E.-K. Dietsche, D. Grosso, S. Haroche, J.-M. Raimond, M. Brune and S. Gleyzes, Nature **535**, 262 (2016); A. Omran, H. Levine, A. Keesling, G. Semeghini, T. T. Wang, S. Ebadi, H. Bernien, A. S. Zibrov, H. Pichler, S. Choi, J. Cui, M. Rossignolo, P. Rembold, S. Montangero, T. Calarco6, M. Endres, M. Greiner, V. Vuletić, M. D. Lukin, Science **365**, 570 (2019); A. Grimm, N. E. Frattini, S. Puri, S. O. Mundhada, S. Touzard, M. Mirrahimi, S. M. Girvin, S. Shankar and M. H. Devoret, Nature **584**, 205 (2020).

[11] S. Haroche, Rev. Mod. Phys. **85**, 1083 (2013); D. J. Wineland, Rev. Mod. Phys. **85**, 1103 (2013).

[12] R. H. Dicke, Phys. Rev. **93**, 99 (1954).

[13] K. D. B. Higgins, S. C. Benjamin, T. M. Stace, G. J. Milburn, B. W. Lovett & E. M. Gauger, Nat. Commun. **5**, 4705 (2014).

[14] R. A. Dourado and M. H. Y. Moussa, Phys. Rev. A **104**, 023708 (2021).

[15] S. Haroche, in New Trends in Atomic Physics, edited by G. Grynberg and R. Stora (North-Holland, Amsterdam, 1983).

[16] L. Moi, P. Goy, M. Gross, J. M. Raimond, C. Fabre, and S. Haroche, Phys. Rev. A **27**, 2043 (1983).

[17] Y. Kaluzny, P. Goy, M. Gross, J. M. Raimond, and S. Haroche, Phys. Rev. Lett. **51**, 1175

(1983).
[18] H. R. Lewis and W. B. Riesenfeld, J. Math. Phys. **9**, 1976 (1969).
[19] S. S. Mizrahi, Phys. Lett. A **144**, 282 (1990).
[20] R. R. Puri and S. V. Lawande, Phys. Lett. A **70**, 69 (1979).
[21] R. Cook, Phys. Rev. A **35**, 3844 (1987).
[22] C. C. Gerry and R. Grobe, Phys. Rev. A **57**, 2247 (1998).
[23] R. J. Cook and A. F. Bernhardt, Phys. Rev. A **18**, 2533 (1978).
[24] S. Inouye, A. P. Chikkatur, D. M. Stamper-Kurn, J. Stenger, D. E. Pritchard, and W. Ketterle, Science **285**, 571 (1999); D. Schneble, Y. Torii, M. Boyd, E. W. Streed, D. E. Pritchard, and W. Ketterle, *ibid.* **300**, 475 (2003); L. Fallani, C. Fort, N. Piovella, M. Cola, F. S. Cataliotti, M. Inguscio, and R. Bonifaci0, Phys. Rev. A **71**, 033612 (2005).
[25] K. Baumann, C. Guerlin, F. Brennecke, and T. Esslinger, Nature **464**, 1301 (2010).
[26] S. Slama, S. Bux, G. Krenz, C. Zimmermann, and P. W. Courteille, Phys. Rev. Lett. **98**, 053603 (2007).
[27] M. D. Lukin, M. Fleischhauer, R. Cote, L. M. Duan, D. Jaksch, J. I. Cirac, and P. Zoller, Phys. Rev. Lett. **87**, 037901 (2001).

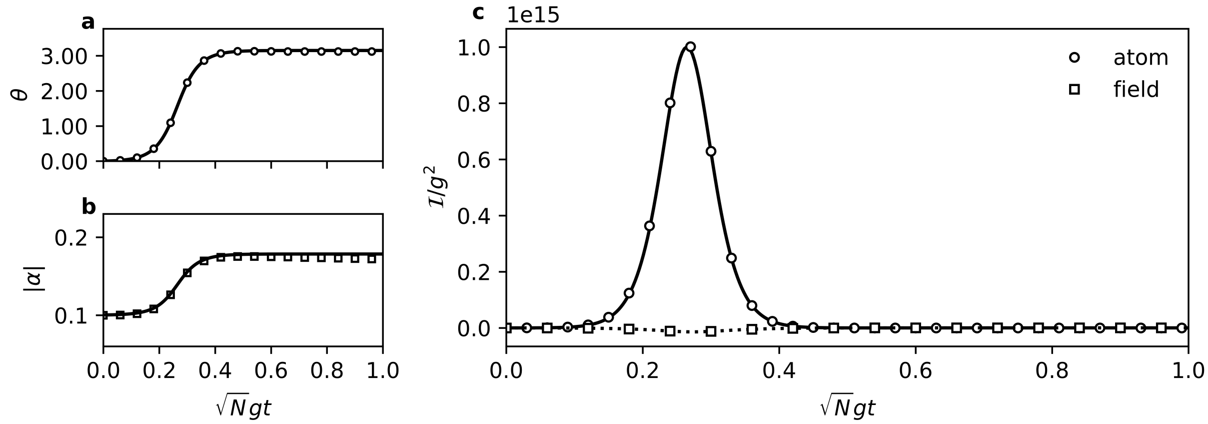

Fig. 1: Plot of the numerical and analytical solutions for (a) $\theta(t)$, (b) $|\alpha(t)|$, (c) $\mathcal{I}_a$ and $\mathcal{I}_f$, against $\sqrt{N}gt$, for the overdamped regime: $\gamma = 4 \times 10^{-2}g$ and $\epsilon = 0.1$. We have assumed $N = 10^6$, $\omega = 10^5 g$, $\alpha_0 = 0.1$, $\theta_0 = 2/N$ and $\phi_0 = \pi/2$. The circles and squares represent the numerical solutions whereas the full and dotted lines represent the analytical ones.

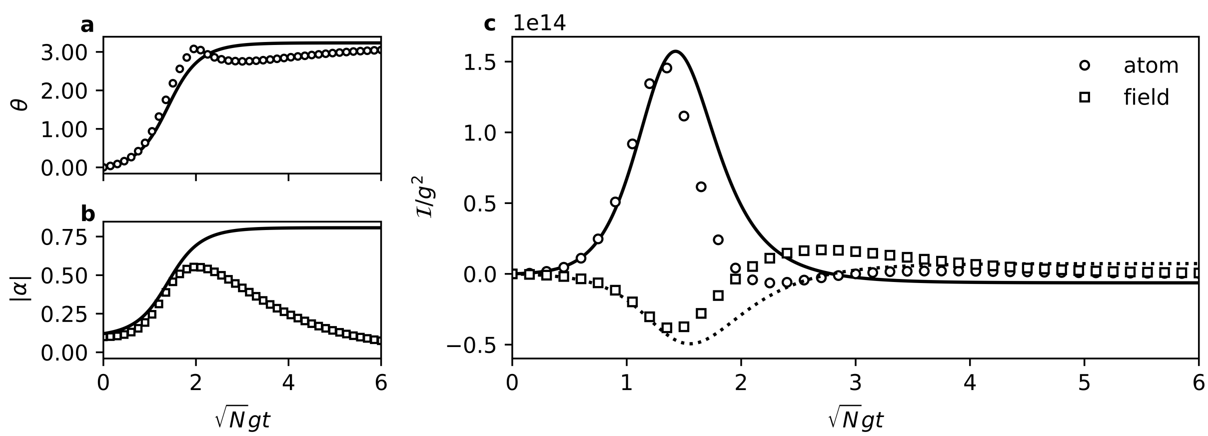

Fig. 2: The same as in Fig. 1 for the damped regime: $\gamma = 4 \times 10^{-3}g$ and $\epsilon = 1$.

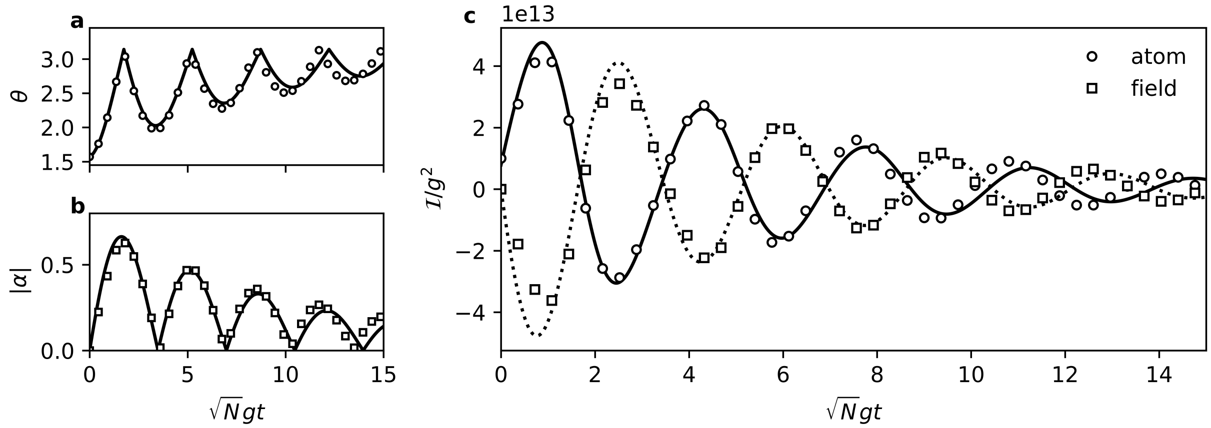

Fig. 3: The same as in Fig. 1 for the underdamped regime: $\gamma = 4 \times 10^{-4} g$ and $\epsilon = 10$.

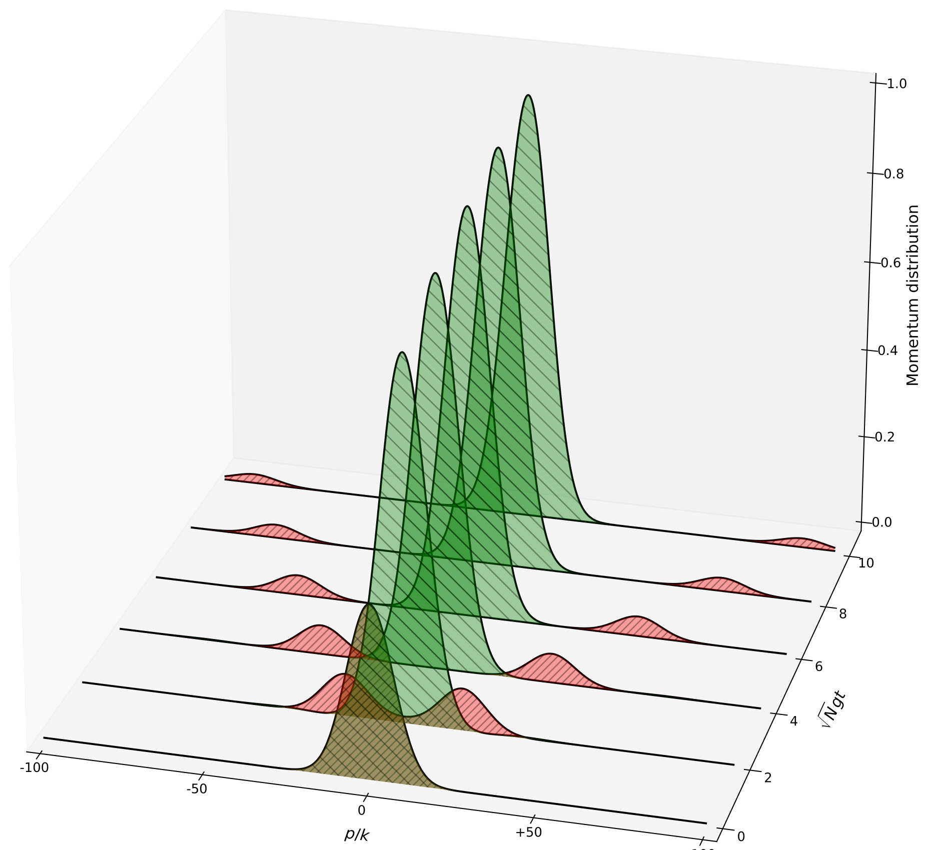

Fig. 4: Plot of the momentum distribution functions $|\mathcal{F}_+|^2$ and $|\mathcal{F}_-|^2$, against $\sqrt{N}gt$, considering the same parameter as in Fig. 3, with $\sigma \approx 0.2/k$. $|\mathcal{F}_+|^2$ and $|\mathcal{F}_-|^2$ are represented by the green and red curves, respectively.